AAS 22-688

MITIGATING THE IMPACT OF MOMENTUM UNLOADS ON STATION-KEEPING AROUND LIBRATION POINT ORBITS

Arianda Farrés* David C. Folta† Cassandra M. Webster‡ and Adam Z. Michaels§

Station-keeping maneuvers are required to maintain a spacecraft close to a Libration point orbit, where the size of these maneuvers depends on different perturbations and any unmodeled forces. In many missions, despite being small, frequent momentum unloads can have a large impact on the size of station-keeping maneuvers. In this paper we will show that applying momentum unloads in the Linear Approximation of the Non-Escape (LANE) direction can significantly reduce their impact on the station-keeping delta-v budget.

INTRODUCTION

Over the past decade, there has been an increased interest in sending spacecrafts to Libration Point Orbits (LPOs), to both the Sun-Earth Libration 1 and 2 (SEL_1 and SEL_2). The location of these two points is ideal for space weather application and deep space observations. Over the next five 5 years NASA is planning several missions to these locations in space, such as the Space Weather Follow On (SWFO) at SEL_1 and the Nancy Grace Roman Space Telescope (RST) at SEL_2. SWFO is a space weather mission that will monitor the Sun for signs of solar storms which may harm the Earth's telecommunication Network. On the other hand, RST is an observatory designed to answer questions about dark energy, exoplanets, and astrophysics.

Periodic and quasi-periodic motion around SEL_1/SEL_2 is unstable, hence station-keeping (SK) strategies are required to cancel this instability and overcome the effect of perturbations and uncertainties. Some of the perturbations come from: orbit determination errors (ODE) where the uncertainties on the position and velocity of the spacecraft affect the size of the planned SK maneuvers; maneuver execution errors (MEE) which will deviate the trajectory from the desired nominal path; solar radiation pressure uncertainties (SRP) due to attitude changes that affect the orbits trajectory between maneuvers; and momentum unloads (MUs) which are small maneuvers performed to desaturate the spacecraft's reaction wheels used for attitude control. These small maneuvers can be very frequent and deviate the spacecraft from the nominal path, impacting on the magnitude of SK maneuvers. In this paper we will focus on the impact of MUs on the station-keeping delta-v

*Dr., NASA/Goddard Space Flight Center, University of Maryland Baltimore County, 8000 Greenbelt Road, Greenbelt, MD 20771.

†Aerospace Engineer, SWFO and Lunar IceCube Navigation and Mission Design Lead, Navigation and Mission Design Branch, NASA/Goddard Space Flight Center, 8000 Greenbelt Road, Greenbelt, MD 20771.

‡Roman Space Telescope (RST) Flight Dynamics Lead, Navigation and Mission Design Branch, NASA/Goddard Space Flight Center, 8000 Greenbelt Road, Greenbelt, MD 20771.

§Navigation and Mission Design Branch, NASA/Goddard Space Flight Center, 8000 Greenbelt Road, Greenbelt, MD 20771.

budget and study how to mitigate their effect. This is of special relevance for SWFO mission, which will experience frequent and large MUs.

We use the Circular Restricted Three Body Problem (CRTBP) as a base model to describe the dynamics of a spacecraft around LPOs as it is a representative model of the true dynamics around SEL_1/SEL_2. The CRTBP also allows us to derive analytical expressions for the directions to perform SK maneuvers and derive alternatives for the MUs directions. We note that when performing analyses to evaluate the impact of the different strategies proposes here we use a higher fidelity force model including the gravitational attraction of all the planets in the solar system, the Moon and SRP.

To understand the impact of maneuvers on the motion around LPOs it is useful to look at the projection of the trajectories in the Floquet Mode (FM) reference frame: a set of periodic or quasi-periodic functions that provide a reference frame, centered at these orbits, where the dynamics can be simplified as a saddle x center x center motion.[1–3] This reference frame has great potential for: (a) understanding and describing the motion around the Libration point orbits; (b) finding minimum delta-v maneuvers to cancel the instability; and (c) understanding the impact of MUs on the orbit's instability. In Reference 3 we studied the relation between the size of the SK maneuvers and the thrust direction, and saw that thrusting along the position components of the stable eigenvector gave the minimum delta-v. Moreover, the FM reference frame allowed us to give a geometrical interpretation to these relations, and to how restrictions on the SK thrust direction impact the station-keeping delta-v budget. We can use the same ideas to study the impact of MUs have on the motion around LPOs and the size of SK maneuvers.

Generally, the direction of MUs is unknown and are modeled as a small maneuver in a random direction. However, in the case of SWFO these will be nominally applied along the Sun-line direction, which has a large impact on the size of SK maneuvers. To mitigate their impact on the size of the SK maneuvers, we propose to change the direction of the MUs, applying them in a direction that does not enhance the instability of the LPO. We use the linearized equation of motion around the LPO to derive the so-called "Escape" and "Non-Escape" directions. Maneuvers in the non-escape directions, at first order, do not add instability to the natural motion. We will see that applying MUs in the non-escape direction significantly reduces the impact on the station-keeping delta-v maneuvers, and for SWFO's support it may eliminate over 90 percent of the station-keeping fuel cost.

SWFO MISSION OVERVIEW

The Space Weather Follow On mission is a ride-share on the SpaceX Falcon 9 launch vehicle carrying NASA's Interstellar Mapping and Acceleration Probe (IMAP) spacecraft. The spacecraft will be operated by the National Oceanic and Atmospheric Administration (NOAA) and will facilitate early warnings for space weather events. SWFO is expected for launch in February 2025, and will orbit the Sun–Earth L1 (SEL_1) Lagrange point. While orbiting around SEL_1, SWFO will collect solar wind data and coronal imagery, the mission will continue the critical measurements from other observatories at SEL_1, such as the Deep Space Climate Observatory (DSCOVR), the Solar and Heliospheric Observatory (SOHO) and the Advanced Composition Explorer (ACE).

In order to meet NOAA's operational requirements to monitor and forecast impacts from solar storm activity, SWFO's trajectory must maintain a Sun-Earth-Vehicle (SEV) angle between 4 and 13 degrees for at least 5 years, which drives the size of the SEL_1 Lissajous mission orbit. The top

plot in Figure 1 shows the transfer trajectory and mission orbit for the mission, where the red and green cones represent the upper and lower bounds for the SEV angle. We note that this constraint is only imposed on the mission orbit. The bottom plot in Figure 1 shows the variation of the SEV as a function of time, the blue line represents the transfer trajectory, the red line the mission orbit and the black dot is the Libration Orbit Insertion (LOI) maneuver location. As we can see, the mission orbit SEV angle remains between 4 and 13 degrees.

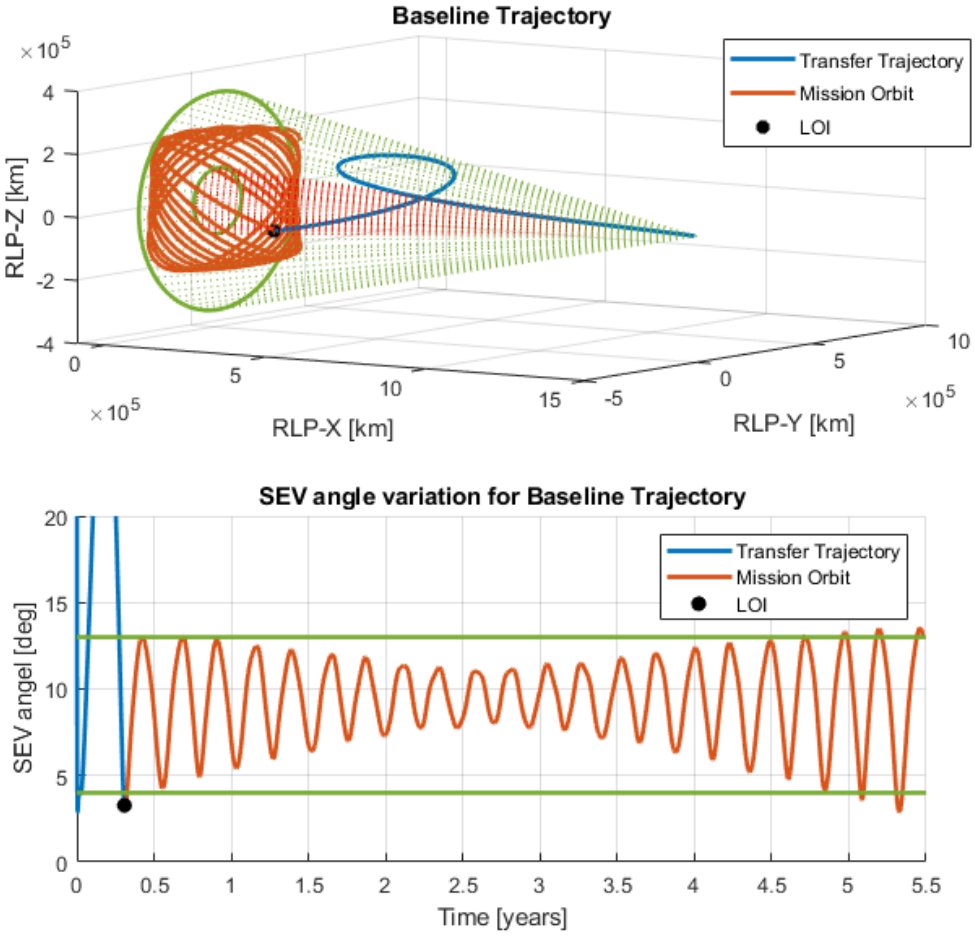

Figure 1. Top: SWFO transfer and mission orbit at SEL_1, Bottom: Variation of the SEV angle for 5 years in the mission orbit.

To cancel the instability of the SEL_1 region and overcome the effect of perturbations and uncertainties SWFO will be performing station-keeping maneuvers every 30 days. The spacecraft will maintain a Sun-pointing attitude during the entire mission, only changing the attitude to perform the SK maneuvers, hence SRP is included in the force model using the cannonball approximation, where no uncertainties due to attitude changes are considered. The only perturbations that have been taken into account in our analysis are ODE and MEE. Finally, due to the spacecraft's design the MUs are every 3 days along the spacecraft-Sun direction with a residual delta-v of approximately 2.5 cm/s.

Station-keeping Strategy

The main goal of a station-keeping maneuver is to ensure that the spacecraft continues to orbit around SEL_1 and remains close to the mission orbit. In the literature we find different approaches to solving this problem, for SWFO we have implemented the so-called velocity constraint at plane crossing approach, which has a long heritage among previous NASA missions like ACE, DSCOVR and most recently the James Webb Space Telescope (JWST).[4]

The strategy is formulated as follows: at the time of the maneuver, find a $\Delta\mathbf{v}$ which ensures that after propagating the trajectory to the 4th $y = 0$ plane crossing the v_x component of the velocity is zero (in the Rotation Libration Point (RLP) reference frame). Thanks to the symmetries in the CRTBP, this condition ensures that the spacecraft is close to a LPO and will continue orbiting around the Libration point over the next two orbital periods. Moreover, if the maneuvers are frequent we can also guarantee that we stay close to the nominal mission orbit.[3]

In order to find the required delta-v maneuver for station-keeping we use a targeting method, where for a fixed thrust direction, $\hat{\mathbf{u}} = \mathbf{u}/||\mathbf{u}||$, we target the maneuver magnitude ($dvmag$) such that if we apply $\Delta\mathbf{v} = dvmag \cdot \hat{\mathbf{u}}$ and propagate the trajectory to the 4th plane crossing, then $v_x = \pm 1 m/s$. Where the sign depends on the location of the spacecraft at the plane crossing relative to SEL_1 ($+$ if the spacecraft is between the SEL_1 and Earth, $-$ if it is between SEL_1 and Sun). This targeting method can be solved with a classical Newton-Raphson method.[3] Note that due to the high instability of the region it is difficult to attempt to find the $dvmag$ by directly targeting the 4th plane crossing. For robustness, it is best to start by finding the $dvmag$ such that $v_x = \pm 1 m/s$ at the 1st plane crossing, and use that as an initial condition for 2nd plane crossing, and follow the same procedure until we reach the 4th plane crossing. Fig. 2 shows a schematic representation of the targeting strategy.

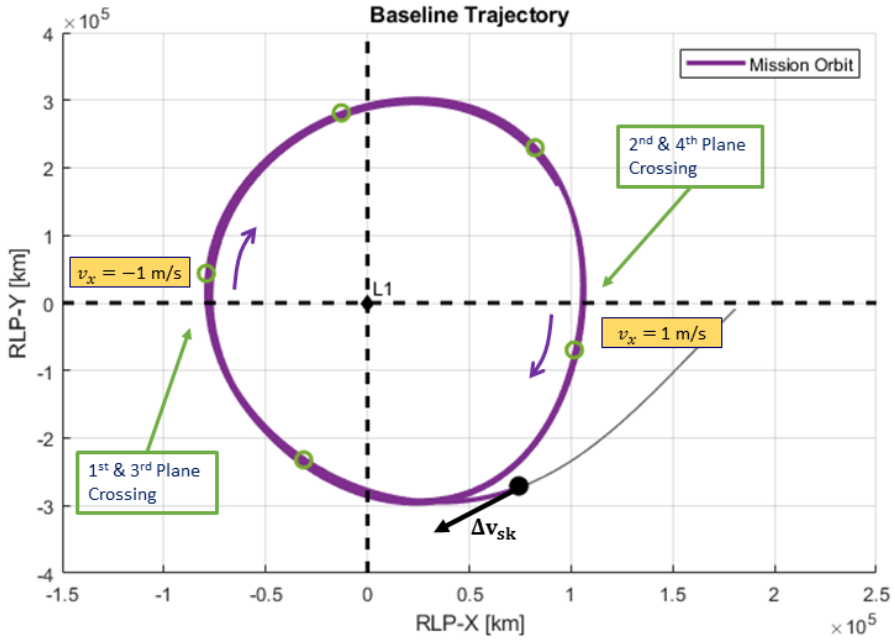

Figure 2. Schematic representation of the targeting method used to derive the SK maneuvers.

The size of the SK maneuvers ($dvmag$) is strictly related to the thrust direction $\hat{\mathbf{u}}$ in which this one is applied. In order to find the minimum thrust direction one could add a minimization scheme to the targeting sequence allowing the thrust direction $\hat{\mathbf{u}}$ to vary. However, from previous studies we know that the minimum thrust direction is aligned with the position components of the stable eigenvector associated to the LPO.[3–6] The stable eigenvector $\mathbf{v}_{stb}$ at the time of the maneuver can be estimated by propagating the trajectories state transition matrix for one orbital period and finding its stable eigenvector. However, one can also use the position components of the stable eigenvector associated to SEL_1 as an approximation, that has the following closed form:

$$\bar{\mathbf{v}}_{stb} = [-2\lambda, \lambda^2 - 2c_2 - 1, 0, \lambda^2 + 2c_2 + 1, -\lambda^3 - (1 - 2c_2)\lambda] \tag{1}$$

where the constant $c_2 = 4.0304$ comes from the linear approximation of the CRTBP equations and $\lambda = 2.5205$ is the real eigenvalue at SEL_1. Hence, take $\mathbf{u} = [-2\lambda, \lambda^2 - 2c_2 - 1, 0]$ as the thrust direction for the station-keeping strategy ($\hat{\mathbf{u}} = \mathbf{u}/||\mathbf{u}||$).

While the direction of the stable and unstable eigenvector associated to a LPO varies along the orbit, they remain close to the stable and unstable eigenvector associated to SEL_1. The left hand side of Fig. 3 shows the variation for two orbital periods of the azimuth and elevation of the stable (green) and unstable (red) directions in the RLP frame. The blue dashed line corresponds to the azimuth and elevation of the $\hat{\mathbf{u}}$ which are $28.25°$ and $0°$ respectively.

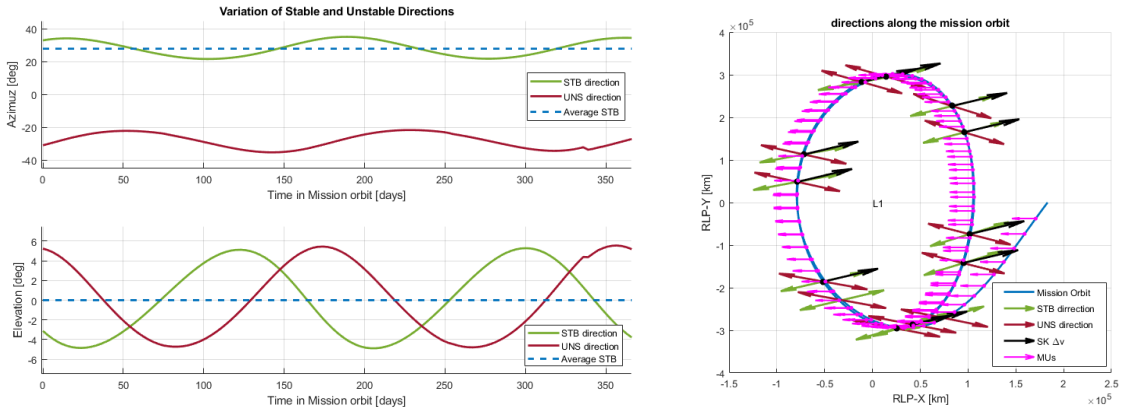

Figure 3. Left: Variation of the Azimuth and Elevation of the stable and unstable eigenvector for one orbital period. Right: Variation of the stable and unstable directions along the mission orbit.

To compare the difference between using the varying stable eigenvector or the SEL_2 eigenvector to determine the SK thrust direction we have performed one year of station-keeping for SWFO with the two different thrust vectors. In both simulations we include MUs every 3 days along the spacecraft-Sun direction with a residual delta-v of 2.5 cm/s. Fig. 4 (top) shows the size of the SK maneuvers as a function of time, the red line represents the size of the SK maneuvers that uses as thrust vector the position components of the SEL_1 stable eigenvector ($\bar{\mathbf{v}}_{stb}$), and the purple line represents the size of the SK maneuvers that uses the Lissajous orbits stable eigenvector ($\mathbf{v}_{stb}$) as thrust direction. Notice how the purple line is slightly below the red line, providing the minimum delta-v maneuvers. Table 1 shows the mean value of the SK maneuvers and the total delta-v for one-year of station-keeping using the two different thrust directions. As we can see the difference in the maneuver magnitudes is less than 0.25 cm/s, which is below the classical 5% maneuver execution

error. The impact on the total delta-v is of 3 cm/s, negligible given that the station-keeping cost is 4.77 m/s. These results show that, from an operational perspective, using the same thrust direction for all SK maneuvers helps simplify the SK strategy, using the SEL_1 stable direction as the thrust direction has a minimal impact on the overall station-keeping delta-v budget.

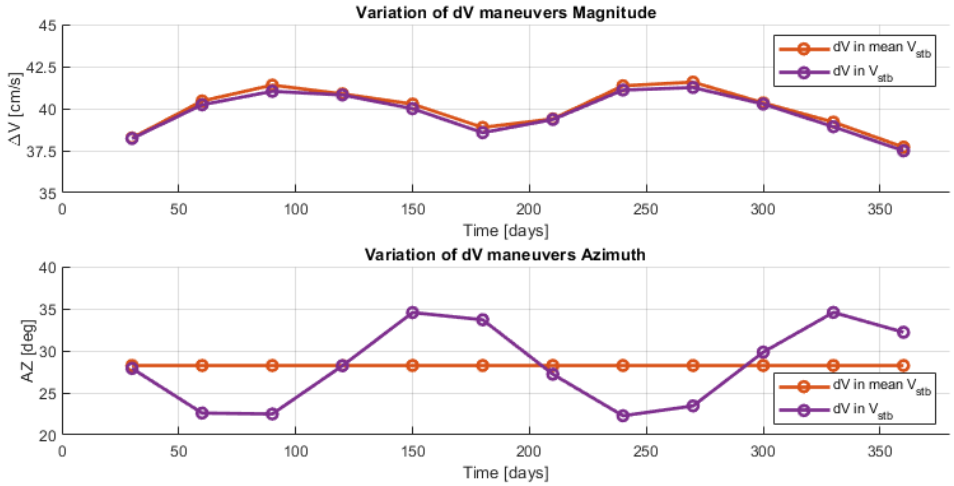

Figure 4. Top: variation of the maneuver magnitudes for one-yer of station-keeping; Bottom: variation of the maneuver azimuth along the mission orbit.

Table 1. Table summarizing the size of the total delta-v for one year of station-keeping and the mean value for a station-keeping maneuver using two different options for the SK thrust direction.

	dV using $\mathbf{v}_{stb}$	dV using $\bar{\mathbf{v}}_{stb}$
Total $\Delta\mathbf{v}$ [m/s]	4.77 m/s	4.80 m/s
Mean SK $\Delta\mathbf{v}$ [cm/s]	39.77 cm/s	39.98 cm/s

Monte Carlo Simulations

In order to asses the main drivers of the station-keeping delta-v budget we have performed several Monte Carlo simulations including ODE and MEE in the simulations. For all the simulations we consider a high fidelity force model that includes the gravitational attraction of the Sun, Earth, Moon and the rest of the planets in the solar system. The force model also considers the SRP acceleration modeled using the cannonball model, given that the spacecraft will always maintain a sun-pointing attitude except during station-keeping maneuvers this is a good approximation.

Maneuver execution errors are applied to the planned station-keeping maneuver, these errors are randomly generated following a normal distribution, considering a 5% maneuver execution errors (3-sigma) and 2.5 degree cone angle error (3-sigma). Orbit determination errors are included to the position and velocity used to plan the delta-v maneuvers using the targeting strategy described above. We have assumed a 10 km 3-sigma normal distribution for the position uncertainties, and 5 cm/s 3-sigma normal distribution for the velocity uncertainties.

In all the simulations SK maneuvers are performed every 30 days along the position component of the Lissajous stable direction at the time of the maneuver ($\mathbf{v}_{stb}$), and MUs performed every 3 days along the spacecraft-Sun direction and a residual delta-v of 2.5 cm/s. We have also included

MEE to the MUs using the same 3-sigma distributions as the SK maneuvers, as both maneuvers are using the same thruster sets in this mission.

We have performed three Monte Carlo simulations, one where we include both MEE and ODE, one where we only include MEE and a third one where we only include ODE. Note that in all simulations MEE are always included for the MUs, and that each Monte Carlo runs contains 1000 different simulations. The idea behind these three Monte Carlo simulations is to determine if either MEE or ODE have a significant impact on the total station-keeping delta-v. Fig. 5 shows histograms of the total station-keeping delta-v for the different cases, where all three cases follow normal distributions with a mean value of 4.77 m/s, the total delta-v for the no error case (see Table 1). The difference between the three different simulations is the 3-sigma intervals, where the upper bound is 5.13 m/s when both ODE and MEE are included, and around 5.03 m/s when either only MEE or ODE are included. The uncertainties in the maneuver execution and orbit determination add up to 36 cm/s to the total delta-v in the worst case scenario.

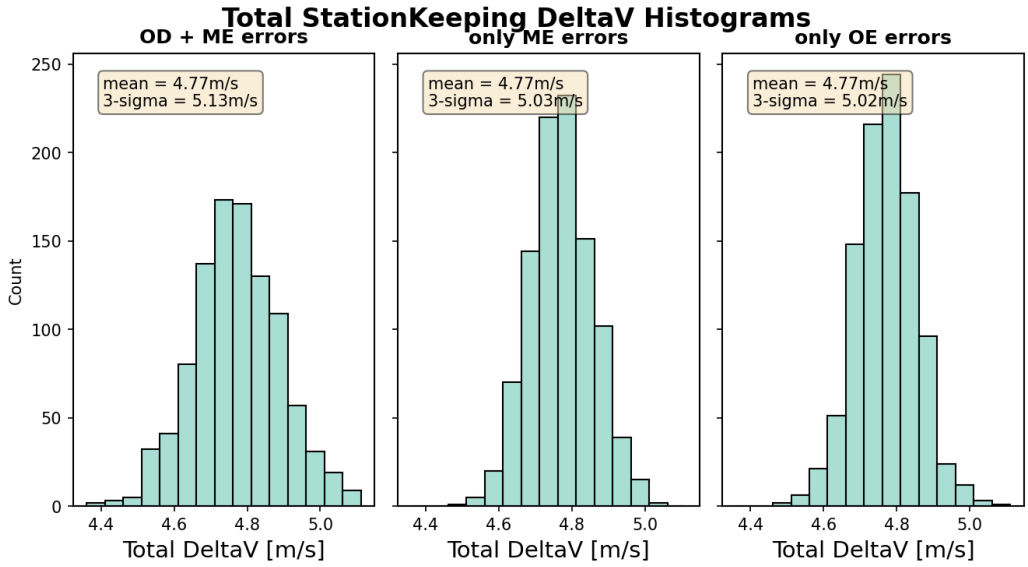

Figure 5. Histograms with the station-keeping total delta-v distribution of 1000 Monte Carlo simulations including MEE and ODE.

It is clear from these results that the main driver of the SK maneuvers are the frequent MUs. We propose to change the direction in which the momentum unloads are applied in order to mitigate the impact of the MUs on the SK maneuvers. The frequent MUs along the spacecraft-Sun direction excite the instability of the Lissajous orbit, resulting in large SK maneuvers. We propose to find directions where maneuvers along those directions have a smaller impact on the natural instability of the orbit.

METHODOLOGY

In order to derive the directions for the momentum unloads (dH) that do not have a large impact on the instability of the orbit in order to reduce the overall delta-v cost to keep SWFO in its mission orbit we use the CRTBP. This allows us to derive analytical expressions for these directions and also get a dynamical understanding of the problem. However, we recall that all the simulations

performed with the different dH directions are done using the high fidelity force model described in the previous section.

Circular Restricted Three Body Problem

It is well known that the CRTBP provides good estimates for the dynamics of the spacecraft in the Sun-Earth/Moon system, and is simple enough to derive some analytical approximations for $\Delta\mathbf{v}$ maneuvers. The CRTBP considers the spacecraft to be a mass-less particle that is affected by the gravitational attraction of two primaries, which are assumed to be point masses evolving around their mutual center of mass in a circular motion. In this case the two primaries are Sun and Earth/Moon barycenter. The equations of motion are derived taking a rotating reference where the origin is at the center of mass of both primaries, and they are both fixed on the X-axis (with the positive side pointing towards the Earth/Moon barycenter); the Z-axis perpendicular to the ecliptic plane and the Y-axis completes an orthogonal positive oriented reference frame. The units of mass, distance, and time are normalized such that the total mass of the system is 1, the Sun-Earth distance is 1 and the period of one Sun-Earth revolution is 2π. The equations of motion are given by:

$$\ddot{X} - 2\dot{Y} = \frac{\partial \Omega}{\partial X}, \qquad \ddot{Y} + 2\dot{X} = \frac{\partial \Omega}{\partial Y}, \qquad \ddot{Z} = \frac{\partial \Omega}{\partial Z}, \tag{2}$$

where, $\Omega(X,Y,Z) = \frac{1}{2}(X^2+Y^2) + \frac{1-\mu}{r_{ps}} + \frac{\mu}{r_{pe}}$, $\mu = 3.0404234 \times 10^{-6}$ is the mass parameter of the system, and $r_{ps} = \sqrt{(X+\mu)^2+Y^2+Z^2}$, $r_{pe} = \sqrt{(X+\mu+1)^2+Y^2+Z^2}$ denotes the relative distances between the spacecraft and the two primaries.

In this paper we focus on the dynamics around SEL_1, however all the derivations also apply around SEL_2, as they both share similar dynamics. We recall that the location of SEL_1 and SEL_2 depends on the value of μ, and their the distance to the small primary (Earth/Moon barycenter) is the only positive solution of the Euler quintic equations:

$$\gamma^5 \mp (3-\mu)\gamma^4 + (3-2\mu)\gamma^3 - \mu\gamma^2 \pm 2\mu\gamma - \mu = 0,$$

where the upper sign corresponds to SEL_1 and the lower to SEL_2.

Linear approximation of motion around SEL_1/SEL_2

To get a first order approximation of the solutions around the SEL_1 and SEL_2 equilibrium we linearize the equations of motion in Eq. 2. Following Reference 7, we center the equations of motion at one of the two equilibrium points and scale the distances such that the distance between the origin (the equilibrium point) and the closest primary (Earth/Moon barycenter) is equal to one. This is done to ensure good numerical properties for the coefficients of higher order expansions. The linearized equations are:

$$\left.\begin{array}{rcl} \ddot{x} - 2\dot{y} &=& (1-2c_2)x \\ \ddot{y} + 2\dot{x} &=& (1-c_2)y \\ \ddot{z} &=& -c_2 z \end{array}\right\} \tag{3}$$

where, $c_2 = \frac{1}{\gamma^3}\left(\mu + (1-\mu)\frac{\gamma^3}{1 \mp \gamma^3}\right)$ is a constant that only depends on the parameter μ, where the upper sign corresponds to SEL_1 and the lower to SEL_2. The solution of the linearized system

(Eq. 3) is:

$$\left.\begin{array}{rcl} x(t) &=& A_1 e^{\lambda t} + A_2 e^{-\lambda t} + A_3 \cos\omega t + A_4 \sin\omega t \\ y(t) &=& cA_1 e^{\lambda t} - cA_2 e^{-\lambda t} + \kappa A_3 \sin\omega t + \kappa A_3 \sin\omega t \\ z(t) &=& A_5 \cos\nu t + A_6 \sin\nu t \end{array}\right\} \tag{4}$$

where A_i are arbitrary constants and c, κ, λ, ω and ν are constants that depend only on c_2, that are given by:

$$\begin{array}{rclcrcl} \lambda &=& \sqrt{\dfrac{c_2 - 2 + \sqrt{9c_2^2 - 8c_2}}{2}}, & \omega &=& \sqrt{\dfrac{2 - c_2 + \sqrt{9c_2^2 - 8c_2}}{2}}, & \nu = \sqrt{c_2}, \\ \kappa &=& \dfrac{-(\omega^2 + 1 + 2c_2)}{2\omega}, & c &=& \dfrac{\lambda^2 - 1 - 2c_2}{2\lambda}. & \end{array}$$

Note that $\pm\lambda, \pm i\omega$ and $\pm i\nu$ correspond to the eigenvalues of the linearized system given by Eq. 3.

The coefficients A_3, A_4, A_5 and A_6 are related to the oscillatory motion which corresponds to the center$\times$center components of the phase space. Solutions with $A_1 = A_2 = 0$ belong to the so-called center manifold, as they only have bounded terms, and they contain the part of the solution corresponding to the pure imaginary eigenvalues. However, when we look at the motion on the center manifold it is more convenient to rewrite the equations using the following relationships $A_3 = A_x \cos\theta, A_4 = A_x \sin\theta$, $A_5 = A_z \cos\psi$ and $A_6 = A_z \sin\psi$. Where the central part of the motion is now expressed as:

$$x(t) = A_x \cos(\omega t + \phi), \qquad y(t) = \kappa A_x \sin(\omega t + \phi), \qquad z(t) = A_z \cos(\nu t + \psi).$$

Using this formulation, the solution on the center manifold are the coupling of two oscillatory motions: one oscillation in the xy components with amplitude A_x; coupled with another oscillation along the z axis of amplitude A_z; both oscillations with different periods ($\omega/2\pi$ and $\nu/2\pi$ respectively). These coupled oscillatory motion represents the Lissajous orbits in the linearized CRTBP, where A_x and A_z are the Lissajous orbit in-plane and out-of-plane amplitudes of the oscillations respectively.

The coefficients A_1 and A_2 determine the exponential part of the solutions, which corresponds to the saddle component of the phase space. A_1 is called the unstable hyperbolic amplitude, because it corresponds with the eigenvalue with positive real part (λ), which is responsible for the orbits instability. On the other hand, A_2 is the stable hyperbolic amplitude as it corresponds to the eigenvalue with negative real part ($-\lambda$) and is related to the stable manifold. For instance, the relation $A_1 = 0, A_2 \neq 0$, defines a stable manifold, as for any orbit verifying this condition the term containing the A_2-component tends to zero, and the trajectory will tend towards the Lissajous orbit defined by A_x and A_z. Similarly, the relation $A_1 \neq 0, A_2 = 0$, defines points on the so-called unstable manifold, where the trajectory escapes from the Lissajous orbit.

From Eq. 4 we can derive the following relations between the trajectories coordinates $(x, y, z, \dot{x}, \dot{y}, \dot{z})$ and the constant A_1, A_2, A_3, A_4, A_5 and A_6:

$$\begin{bmatrix} x \\ y \\ \dot{x} \\ \dot{y} \end{bmatrix} = \begin{bmatrix} e^{\lambda t} & e^{-\lambda t} & \cos\omega t & \sin\omega t \\ ce^{\lambda t} & -ce^{-\lambda t} & \kappa \sin\omega t & -\kappa \cos\omega t \\ \lambda e^{\lambda t} & -\lambda e^{-\lambda t} & -\omega \sin\omega t & \omega \cos\omega t \\ c\lambda e^{\lambda t} & -c\lambda e^{-\lambda t} & \kappa\omega \cos\omega t & -\kappa\omega \sin\omega t \end{bmatrix} \begin{bmatrix} A_1 \\ A_2 \\ A_3 \\ A_4 \end{bmatrix}, \tag{5}$$

$$\begin{bmatrix} z \\ \dot{z} \end{bmatrix} = \begin{bmatrix} \cos\nu t & \sin\nu t \\ -\nu \sin\nu t & \nu \cos\nu t \end{bmatrix} \begin{bmatrix} A_5 \\ A_6 \end{bmatrix}. \tag{6}$$

Linear Approximation of the Escape and Non-Escape directions

By inverting Eq. 5 one can get the constants A_1 and A_2, associated to the unstable and stable manifolds, as a function of the trajectory coordinates $(x(t), y(t), z(t), \dot{x}(t), \dot{y}(t), \dot{z}(t))$ at a given time t :

$$\begin{bmatrix} A_1 \\ A_2 \end{bmatrix} = \begin{bmatrix} \frac{-\kappa\omega}{2d_1}e^{-\lambda t} & \frac{\omega}{2d_2}e^{-\lambda t} & \frac{\kappa}{2d_2}e^{-\lambda t} & \frac{1}{2d_1}e^{-\lambda t} \\ \frac{-\kappa\omega}{2d_1}e^{\lambda t} & \frac{-\omega}{2d_2}e^{\lambda t} & \frac{-\kappa}{2d_2}e^{-\lambda t} & \frac{1}{2d_1}e^{\lambda t} \end{bmatrix} \begin{bmatrix} x \\ y \\ \dot{x} \\ \dot{y} \end{bmatrix}, \tag{7}$$

where $d_1 = c\lambda - \kappa\omega$ and $d_2 = c\omega + \kappa\lambda$ (further details in Reference 8).

Let us assume that we are on a trajectory that verifies the non-escape condition $A_1 = 0$, i.e. the trajectory is on, or tends towards the Lissajous orbit. Using Eq. 7, the non-escape condition is equivalent to having $(x, y, \dot{x}, \dot{y})$ satisfy:

$$\frac{k}{d_2}\dot{x} + \frac{1}{d_1}\dot{y} = \frac{k\omega_1}{d_1}x - \frac{\omega_1}{d_2}y. \tag{8}$$

Let us then consider the trajectory after a delta-v maneuver $(x, y, z, \dot{x} + \Delta\dot{x}, \dot{y} + \Delta\dot{y}, \dot{z} + \Delta\dot{z})$ and impose that it also satisfies the non-escape condition $A_1 = 0$. As a result, the non-escape condition (Eq. 8) is kept for maneuvers $[\Delta\dot{x}, \Delta\dot{y}, \Delta\dot{z}]$ along the $\mathbf{s} = \pm[d_2, -kd_1, 0]$ direction. While for maneuvers along the $\mathbf{u} = \pm[kd_1, d_2, 0]$ direction the escape condition is maximized (i.e., note that $\mathbf{s} \perp \mathbf{u}$).

Notice that the non-escape directions ($\hat{\mathbf{s}} = \pm\mathbf{s}/||\mathbf{s}||$) are good for applying the MUs residuals, as they have no impact on the instability of the orbit in the linearized system, and will have a small impact in the non-linear system. While maneuvers along the escape directions ($\hat{\mathbf{u}} = \pm\mathbf{u}/||\mathbf{u}||$) are good for SK, because a small delta-v along that direction has a significant change along the unstable manifold. It is worth noting that the escape direction $\mathbf{u} = \pm[kd_1, d_2, 0]$ is parallel to the position components of the SEL_1 stable eigenvector $\bar{\mathbf{v}}_{stb} = [-2\lambda, \lambda^2 - 2c_2 - 1, 0]$ introduced in the previous section. Where we saw that performing SK maneuvers along this direction instead of the stable direction at the time of the maneuver had a small impact on the overall delta-v budget.

Fig. 6 shows the relation between these different directions in the RLP reference frame centered at SEL_1. As we can see the SEL_1 stable direction and escape direction coincide, while the non-escape direction is 61.75 degrees off the spacecraft-Sun direction and perpendicular to the escape direction. While the SEL_1 stable and unstable directions are ± 28.25 degrees off the spacecraft-Sun direction. Finally, we recall that in Reference 3 we used the Floquet Mode reference frame to derive the minimum-thrust direction for the station-keeping of Halo orbits, using the same idea, derive a maneuver that maximized the change along the unstable mode.

Proposed dH/dV strategy

We recall that the current nominal plan for SWFO is to perform the momentum unloads (dH) along the spacecraft-Sun direction to maximize the time we are observing the Sun, and the station-keeping maneuvers (dV) along the direction defined by the position components of the stable eigenvector. In order to mitigate the impact of the momentum unloads on the station-keeping delta-v budget we propose to use the non-escape direction ($\hat{\mathbf{s}}$) for dH, as these are frequent maneuvers and we want to avoid deviating from the Lissajous pattern, and use the escape directions ($\hat{\mathbf{u}}$) for dV, as we want to maximize the change along the unstable manifold to get back to the Lissajous orbit with

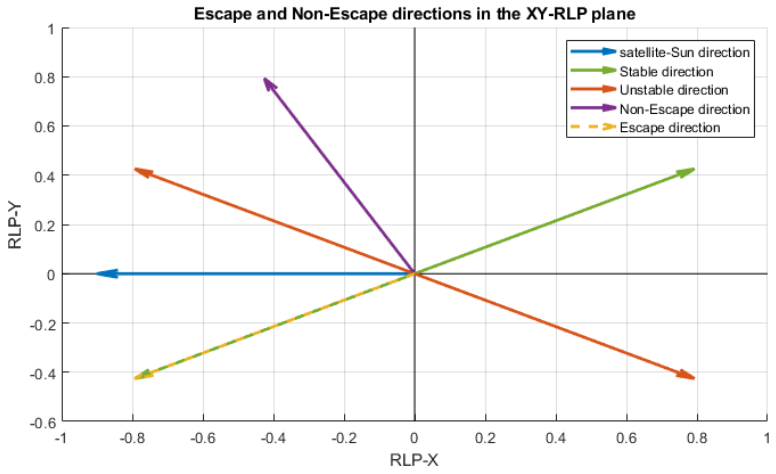

Figure 6. Representation of the spacecraft-Sun direction, the stable and unstable directions, and the escape and non-escape directions in the RLP reference frame at SEL_1.

minimum delta-v. Fig. 7 shows a schematic representation of these two dH/dV sequences along the mission orbit.

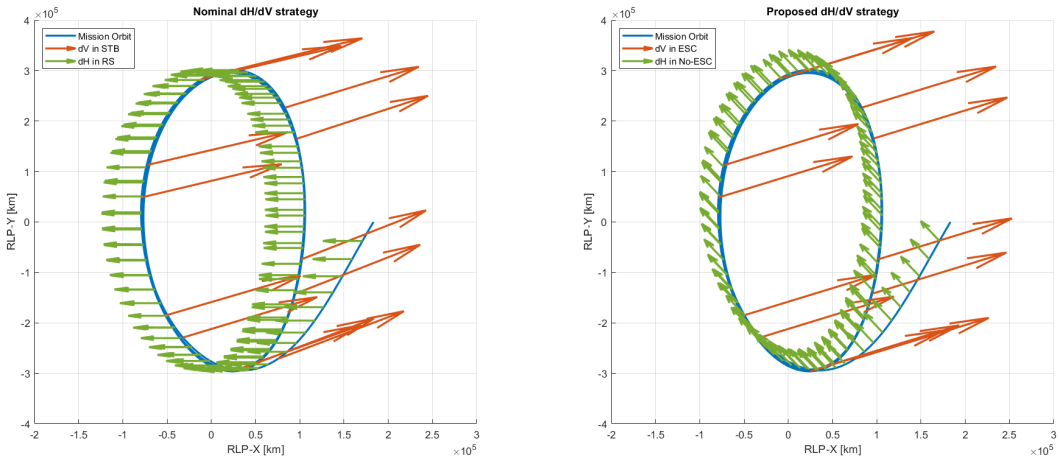

Figure 7. Relation between the dH/dV directions along the Lissajous orbit pattern. Left: Nominal case where the dH is along the spacecraft-Sun line and dV along the stable direction; Right: Proposed case where the dH are along the non-escape direction ($\hat{\mathrm{s}}$), and dV along the escape direction ($\hat{\mathrm{u}}$).

As we know, while moving along the Lissajous orbit, the stable and unstable directions vary (see Fig. 3), and so do the escape and non-escape directions. In order to account for this, we could approximate the non-escape direction by a direction perpendicular the stable eigenvector and contained in the ecliptic plane. In the next section we analyze the impact of this proposed dH/dV strategy on the total delta-v for station-keeping.

RESULTS

In this section we study how much the station-keeping delta-v cost varies when we change the direction in which the momentum unloads are applied. We will look at two different scenarios, first applying the MUs along the non-escape direction derived in the previous section, second applying the MUs along a range of directions between the spacecraft-Sun direction (RS) and the linear approximation of the non-escape (LANE) direction. We compare these results with the nominal case, where the MUs are applied along RS. For all simulations, as it was done for the nominal case, the SK maneuvers are applied every 30 days along the stable direction, and the MUs every 3 days with a residual delta-v of 2.5 cm/s. We assume that the residual delta-v is the same regardless of the MUs direction.

Fig. 8 shows the direction of the MUs (dH maneuvers) relative to the stable and unstable directions for different cases that have been studied, in both plots all directions are centered at the origin. On the left hand side, we can see how the variations of the stable (green) and unstable (red) directions, as well as the variation of the non-escape direction (yellow) and the purple arrow represents the LANE direction. On the right hand side, we have the stable (dashed green) and unstable (dashed red) direction associated to SEL_1, and the range of directions used in the simulations between RS and the LANE direction.

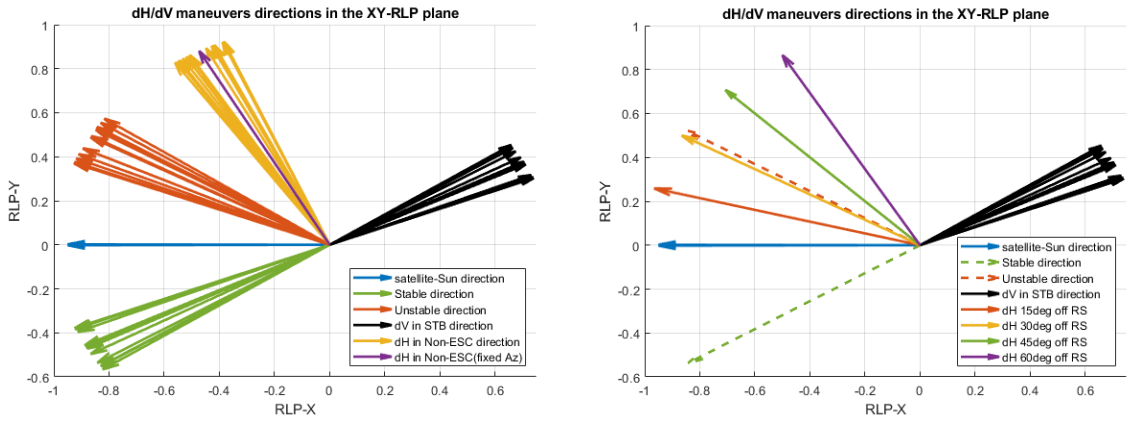

Figure 8. Relation between the directions to apply the dH maneuvers and the stable and unstable directions for the different simulations. Left: dH maneuvers in the non-Escape direction; Right: scan different dH directions between spacecraft-Sun direction and the linear approximation of the non-escape direction.

Momentum Unload along the Non-escape direction

In the previous section we proposed to perform all the MUs along the linear approximation of non-escape direction ($\hat{u}$). However, as mentioned in the previous sections this direction varies as we move along the Lissajous orbit, and can be approximated by a perpendicular direction to the direction defined by the position component of the stable eigenvector. For this first analysis run the following scenarios:

1. dH **in non-escape direction with fixed Azimuth**: case in which the MUs are applied along the LANE direction, given by the vector ($\hat{\mathbf{s}}$) derived in the previous section. We recall that this direction is 61.75 degrees off RS.

2. dH **in non-escape direction with varying Azimuth**: case in which the MUs are applied along the non-escape direction, that is kept fixed between SK maneuvers. For each SK interval the non-escape direction is approximated by a vector perpendicular to the position components of $\mathbf{v_{stb}}$ that is contained in the ecliptic plane ($z = 0$). We can either consider the stable direction at the time of the SK maneuver (option 1) or the mean stable direction between two SK maneuvers (option 2).

Fig. 9 (top) shows the size of the SK maneuvers as a function of time, for the three different scenarios described above. The purple line corresponds to the scenario where the MUs are along the LANE direction, while the yellow and light blue corresponds to the scenarios where the MUs direction changes between SK maneuvers (options 1 and 2 respectively). As we can see the results improve if we change the direction of the MUs along the mission orbit, to better approximate the non-escape direction. However, in all three scenarios the size of the SK maneuvers have been drastically reduced. Recall that in the nominal case (Table 1) the average size of the SK maneuvers was 39.77 cm/s, while in all three scenarios the size of the SK maneuvers is always below 9 cm/s. Having reduced the average size of the SK maneuvers more than 30 cm/s. The bottom plot of Fig. 9 shows the Azimuth variation of the MUs for each of the three scenarios.

Table 2 summarizes the mean value of the SK maneuvers and the total delta-v for one-year of station-keeping for these three scenarios, as well as the nominal case (MUs along RS) for comparison. As we can see, even for the scenario where the MUs are along the LANE direction the total station-keeping delta-v is reduce more than 90%, as well as the size of the average SK maneuvers that goes from 39.77 cm/s to 3.34 cm/s. In the scenarios in which the MUs is adjusted between SK maneuvers the reduction of the delta-v cost is of more than 95%.

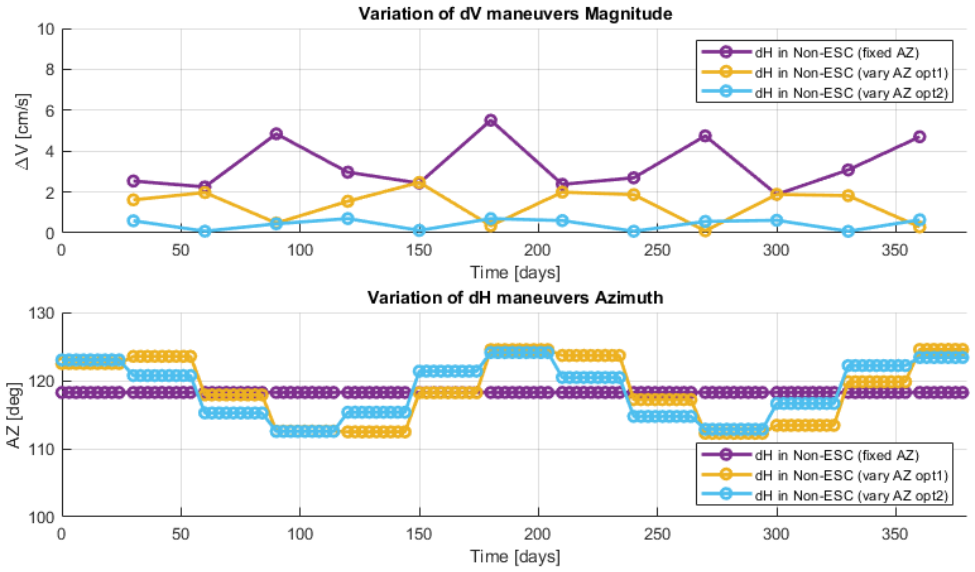

Figure 9. For simulations with dH along the non-escape direction. Top: variation of the maneuver magnitudes for one-year of station-keeping; Bottom: variation of the maneuver azimuth along the mission orbit

Table 2. Table summarizing the size of the total delta-v for one year of station-keeping and the mean value for a station-keeping maneuver for the different non-escaped options for the dH direction.

	dH in RS	dH in Non-ESC (fixed Az)	dH in Non-ESC (vary Az opt1)	dH in Non-ESC (vary Az opt2)
Total Δv [m/s]	4.77 m/s	0.40 m/s	0.16 m/s	0.05 m/s
Mean SK Δv[cm/s]	39.77 cm/s	3.34 cm/s	1.37 cm/s	0.44 cm/s

Momentum Unload along different fixed directions

Let us now check how the station-keeping delta-v is affected when we consider the MUs along different fixed directions. We consider different fixed dH directions between RS (Azimuth of 180 deg) and the LANE direction (Azimuth of 118.25 deg). We expect the size of the SK maneuvers to decrease as we move from RS to LANE. The idea of this scan is to address the cases in which the MUs have some limitations regarding of the slew times between a Sun-pointing attitude and a LAME attitude for the momentum unload dumps.

The top plot in Fig. 10 shows the variation of the size of the SK maneuvers as a function of time, and the bottom plot of the same figure shows the corresponding azimuth variation for each of the analyzed cases. As we can see on the top plot, the size of the SK maneuvers drops by $\approx$ 9 cm/s every 15 degree increase on the angle between RS and the MUs, having all SK maneuvers below 20 cm/s for dH 45 degrees away from RS.

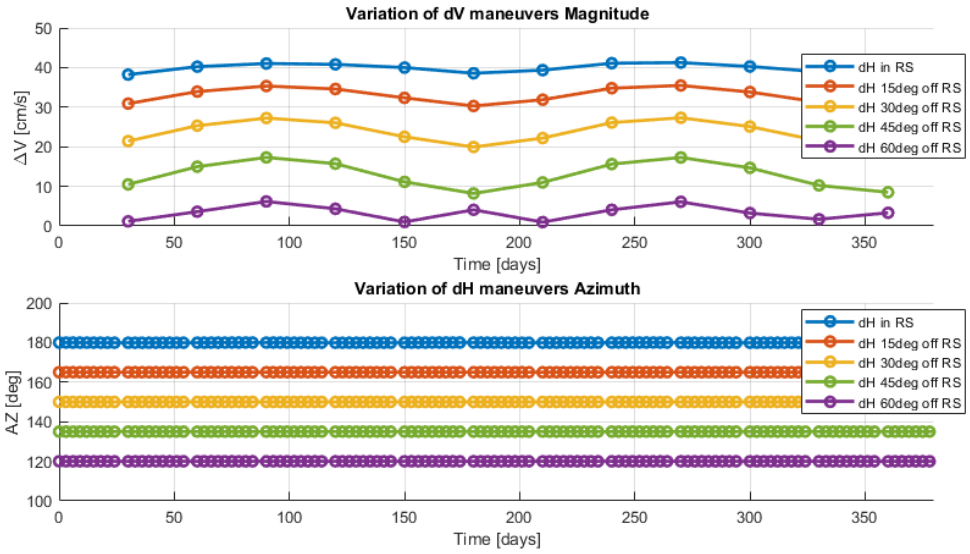

Figure 10. For simulations with different dH directions between RS and LANE. Top: variation of the maneuver magnitudes for one-yer of station-keeping; Bottom: variation of the maneuver azimuth along the mission orbit

Table 3 summarizes the mean value of the SK maneuvers and the total delta-v for one-year of station-keeping for the scanned cases, as well as the nominal case (MUs along RS) for comparison. As we can see, the total delta-v is almost halved for the dH 30 degrees away from RS case, and goes below 2 m/s for the dH 45 degrees away from RS, showing the significant impact we can have on the SK maneuvers if we change the direction of the MUs.

Table 3. Table summarizing the size of the total delta-v for one year of station-keeping and the mean value for a station-keeping maneuver for the different dH directions between RS and LANE.

	dH in RS	dH 15 deg off	dH 30 deg off	dH 45 deg off	dH 60 deg off
Total $\Delta\mathbf{v}$ [m/s]	4.77 m/s	3.94 m/s	2.84 m/s	1.55 m/s	0.40 m/s
Mean SK $\Delta\mathbf{v}$[cm/s]	39.77 cm/s	32.86 cm/s	23.70 cm/s	12.93 cm/s	3.31 cm/s

Monte Carlo Simulations

We have performed Monte Carlo simulations including orbit determination and maneuver execution errors in the simulations for two of the best dH/dV strategies to mitigate the impact of MUs on the station-keeping delta-v, where each Monte Carlo runs contains 1000 different simulations. The first scenario (`dHdV_fixed`) considers the dH maneuvers along the LANE direction ($\mathbf{u}$) and the dV maneuvers along the escape direction ($\mathbf{s}$) (i.e, recall that this is the same direction as the stable eigenvector of SEL_1). The second scenario (`dHdV_vary`) considers the dH maneuvers along the mean non-escape direction between SK maneuvers and the dV maneuvers along the position components of the stable eigenvector at the time of the maneuver. We compare these two scenarios to the Monte Carlo simulations performed for the current nominal case analyzed before, where the dH maneuvers are along the spacecraft-Sun direction. All the simulations SK maneuvers are performed every 30 days and MUs performed every 3 days with a residual delta-v of 2.5 cm/s.

We recall that the Monte Carlo runs include MEE that are applied to the planed station-keeping maneuver and DE that are added to the position and velocity used to plan the delta-v maneuvers using the targeting strategy. The MEE are randomly generated following a normal distribution, considering a 5% maneuver execution errors (3-sigma) and 2.5 degree cone angle error (3-sigma), while for the ODE we have assumed a 10 km 3-sigma normal distribution for the position uncertainties, and 5 cm/s 3-sigma normal distribution for the velocity uncertainties.

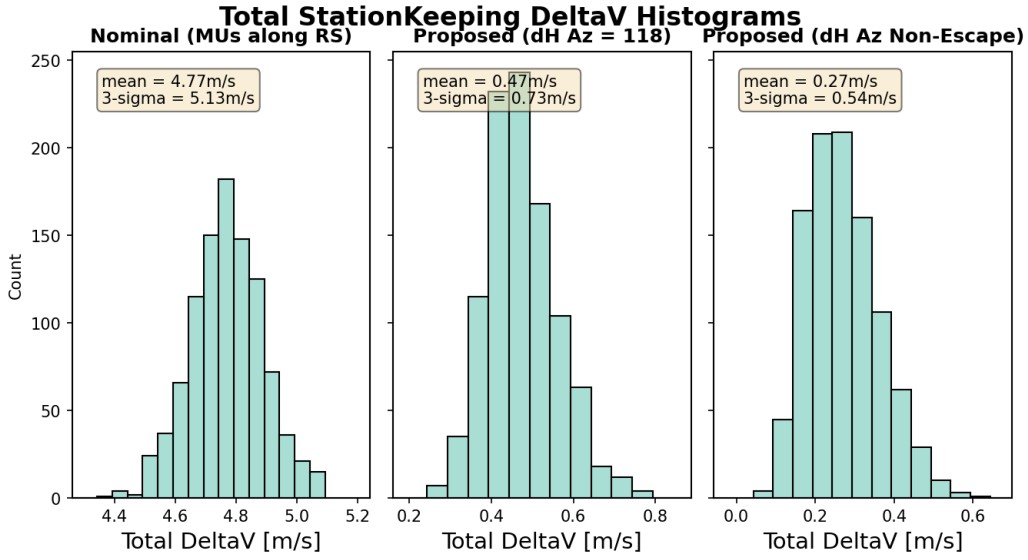

Figure 11. Histograms with the station-keeping total delta-v distribution of 1000 Monte Carlo simulations including MEE and ODE.

Fig. 11 shows histograms of the total station-keeping delta-v for the different scenarios, where

we can see that all three cases follow normal distributions. The mean value for the nominal case is 4.77 m/s, and the two proposed dH/dV strategies have a much smaller mean value for case `dHdV_fixed` is 0.47 m/s and for case `dHdV_vary` is 0.27 m/s. For the three simulated cases the upper bound for the 3-sigma distribution is of 5.13 m/s, 0.73 m/s and 0.54 m/s respectively. Having a reduction of almost 85% using dH/dV strategy in the `dHdV_fixed` case and of almost 90% using the dH/dV strategy in the `dHdV_vary` case. Hence, changing the direction in which the momentum unloads are applied can help mitigate the impact of the MUs on the SK maneuvers and drastically reducing the overall station-keeping delta-v.

GEOMETRIC INTERPRETATION

In the previous section we saw that changing the direction of the MUs can have a large impact on the size of the station-keeping maneuver. As we studies, applying the MUs close to the non-escape direction can drastically reduce the size of the SK maneuvers, as the non-escape direction does not deviate the trajectory along the unstable direction. To understand the differences between the dH/dV strategies simulated in the previous section, we have to look at the projection of the spacecraft trajectory and maneuver directions on the saddle plane[3] (i.e., the plane generated by the stable and unstable directions).

As we know, the linear dynamics around SEL_1 is saddle×center×center, and so is the linear behavior around a small Lissajous orbit.[8] To describe the motion close to a Lissajous orbit one should derive the quasi-periodic Floquet Mode reference frame, in the same way it is done for Halo orbits.[1–3] For the purpose of this study, as we are considering small Lissajous orbits, one can also use the linear approximation of the equations of motion at SEL_1 and derive a reference frame that splits the motion into a saddle and the two center planes (the SCC reference frame from now on) and use this reference frame to describe how different maneuver directions impact the spacecrafts trajectory. The SCC reference frame is defined by the eigenvalues of the linearized equations of motion.

The change of variables, $\xi = C\eta$, between the RLP and the SCC reference frames can be found as follows. Let us start by taking the linearized equations of motion around SEL_1 given by Eq. 3, that can be expressed as $\dot{\xi} = A\xi$, with $\xi = (x, y, z, \dot{x}, \dot{y}, \dot{z})$. Where $\pm\lambda, \pm i\omega$ and $\pm i\nu$ are the eigenvalues of A and $\mathbf{v}_\lambda$, $\mathbf{v}_{-\lambda}$, $\mathbf{u}_\omega = \mathbf{u}_\omega^{\mathbf{re}} \pm i\mathbf{u}_\omega^{\mathbf{im}}$ and $\mathbf{u}_\nu = \mathbf{u}_\nu^{\mathbf{re}} \pm i\mathbf{u}_\nu^{\mathbf{im}}$ are their associated eigenvalues. We define C as the matrix that has as columns the vectors $\mathbf{v}_\lambda, \mathbf{v}_{-\lambda}, \mathbf{u}_\omega^{\mathbf{re}}, \mathbf{u}_\omega^{\mathbf{im}}, \mathbf{u}_\nu^{\mathbf{re}}$ and $\mathbf{u}_\nu^{\mathbf{im}}$. One can see that C is invertible and satisfies $D = C^{-1}AC$, where D can be written as,

$$D = \left[\begin{array}{cc|cc|cc} \lambda & 0 & & & & \\ 0 & -\lambda & & & & \\ \hline & & 0 & \omega & & \\ & & -\omega & 0 & & \\ \hline & & & & 0 & \nu \\ & & & & -\nu & 0 \end{array}\right].$$

The linearized equations of motion are expressed as $\dot{\eta} = D\eta$ after applying the change of variables $\xi = C\eta$, where we $\eta = (e_1, e_2, e_3, e_4, e_5, e_6)$. The solution of the equations of motion in the SCC reference frame is simple: on the plane generated by $\{e_1, e2\}$ the motion is a saddle, and the trajectory escapes with an exponential rate along the unstable direction; and on the planes generated

by $\{e_3, e_4\}$ and $\{e_5, e_6\}$ the dynamics consists of a rotation of period $\omega/2\pi$ and $\nu/2\pi$ respectively. Fig. 12 shows a schematic representation of the solutions around SEL_1 using the SCC reference frame.

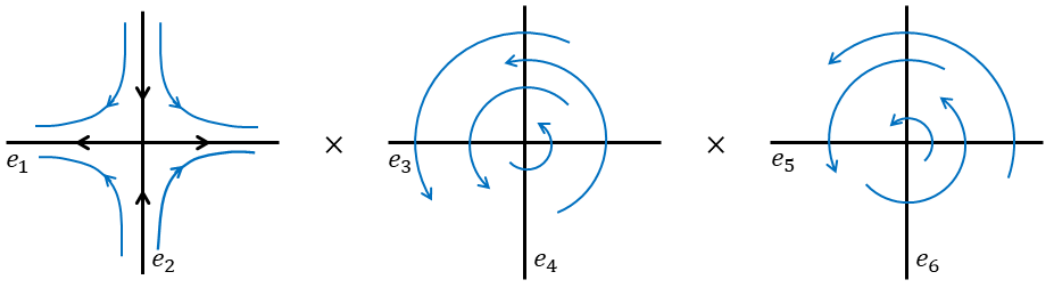

Figure 12. schematic representation of the dynamics around a halo orbit using the SCC reference frame $\overline{e}_i(t)$

We use the SCC reference frame to describe the behaviour of the different dH/dV strategies presented in the previous sections, paying special attention on the projection of the trajectories on the saddle plane (i.e., plane generated by $\{e_1, e_2\}$). We recall that delta-v maneuvers are modeled as instantaneous changes in the velocity and they can be seen as jumps on the phase space. Before showing their impact on the trajectory let us discuss how the RS, escape ($\hat{\mathbf{u}}$) and non-escape ($\hat{\mathbf{s}}$) directions are projected on the saddle plane. Note that these are vectors in $\mathbb{R}^3$ hence the vectors we apply the change of variables defined by $\xi = C\eta$ and project on the saddle planes are: $(0_{1\times 3}, \text{RS})$, $(0_{1\times 3}, \hat{\mathbf{u}})$ and $(0_{1\times 3}, \hat{\mathbf{s}})$. Fig. 13 shows the projection of these three directions, as well as the directions defined by the position components of the stable and unstable vectors in the RLP reference frame (left) and the SCC reference frame (right). As we can see, the projection the non-escape direction (purple line) in the SCC reference frame has no component in the unstable direction e_1 of the saddle plane, hence maneuvers in that direction do not add instability to the spacecraft's trajectory, however this one will continue to deviate along the unstable direction due to the natural saddle dynamics. On the other hand, maneuvers along RS and $\hat{\mathbf{u}}$ move the spacecraft's trajectory away from the stable direction (e_2) adding to the natural instability of the orbit.

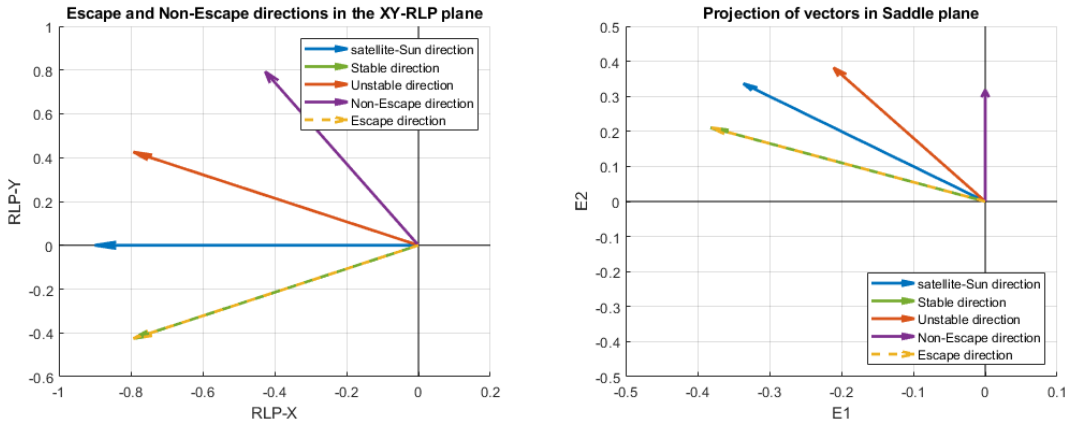

Figure 13. The spacecraft-Sun direction (RS), the stable and unstable directions, and the escape ($\hat{\mathbf{u}}$) and non-escape ($\hat{\mathbf{s}}$) directions in the RLP-XY (left) and saddle plane (right).

Let us now show how the trajectory of the spacecraft looks on the saddle plane projection for two different dH/dV strategies: nominal SWFO strategy (dH along the spacecraft-Sun direction RS) vs the one proposed in this paper (dH along the non-escape direction $\hat{\mathbf{s}}$). In both cases the dV maneuvers are along the escape direction $\hat{\mathbf{u}}$. For this example we have taken the linearized equations of motion, set a random initial condition close to the Lissajous orbits, and propagated the trajectories applying the two different dH/dV strategies. Where the dH maneuvers are applied every 3 days with a residual delta-v of 2.5 cm/s, and the dV maneuvers are applied every 30 days with the size computed to cancel the instability (i.e. bring the trajectory back to $e_1 = 0$). We know that the size of a station-keeping maneuver is related to the distance between the spacecraft and the nominal orbit along the unstable direction, and the thrust direction of the maneuvers.[3] Given that all dV maneuvers are applied along the same direction, the size will be only related to position along e_1 in the saddle plane at the time of the maneuver.

Fig. 14 shows the projection of both trajectories on the saddle plane. The left plot shows the case where dH along RS, and the right plot shows the case when dH is along the non-escape direction. In both plots the magenta lines represent the dH maneuvers and the green arrows the dV maneuvers,while the spacecraft trajectory is represented in blue (nominal case) and red (proposed case). As we can see, applying the momentum unloads along RS makes the trajectory escape faster along e_1 resulting on a larger magnitude for the dV maneuvers.

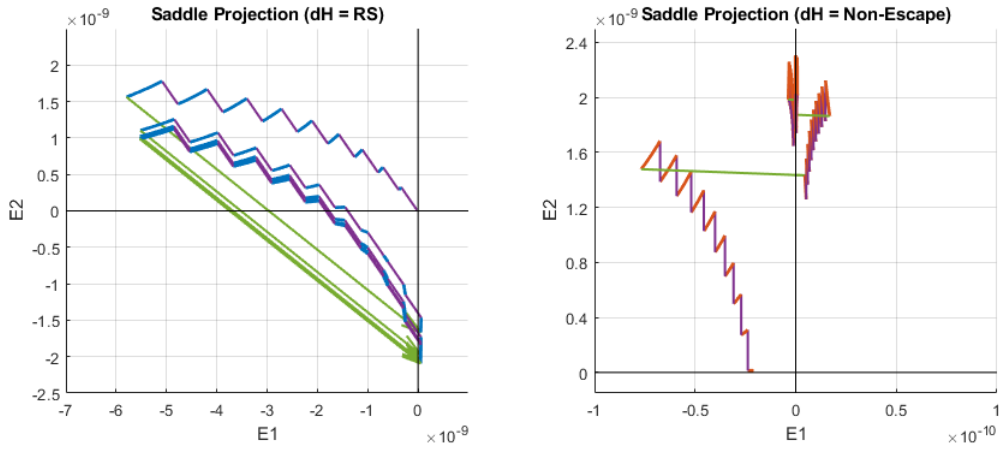

Figure 14. Projection of the trajectory on the saddle plane for different dH/dV strategies, dH along RS (left) and dH along the non-escape direction (right). In both plots, the purple lines represent the dH maneuveres and the green lines the dV maneuvers. The spacecraft's trajectory for the corresponding dH/dV is represented in blue (left) and red (right).

The same analyses can be done for scenarios summarized in Table 3, where the dH maneuvers are applied along a range of different directions between RS and $\hat{\mathbf{s}}$. The scenarios considered took dH 15, 30, 45 and 60 degrees off the spacecraft-Sun line, and as we can see in Table 3 the size of the station-keeping maneuvers decreases as dH gets closer to the non-escape direction that is 61,75 degrees off the satellite-Sun line. Fig. 15 shows the projection of these four new scenario (from top to bottom and left to right cases dH 15, 30, 45 and 60 degrees off RS). As we can see, as the projection of the dH maneuver on the saddle plane gets closer the non-escape direction, the trajectory experiences a smaller excursion along the unstable direction (e_1) resulting on smaller dV maneuvers (green arrow).

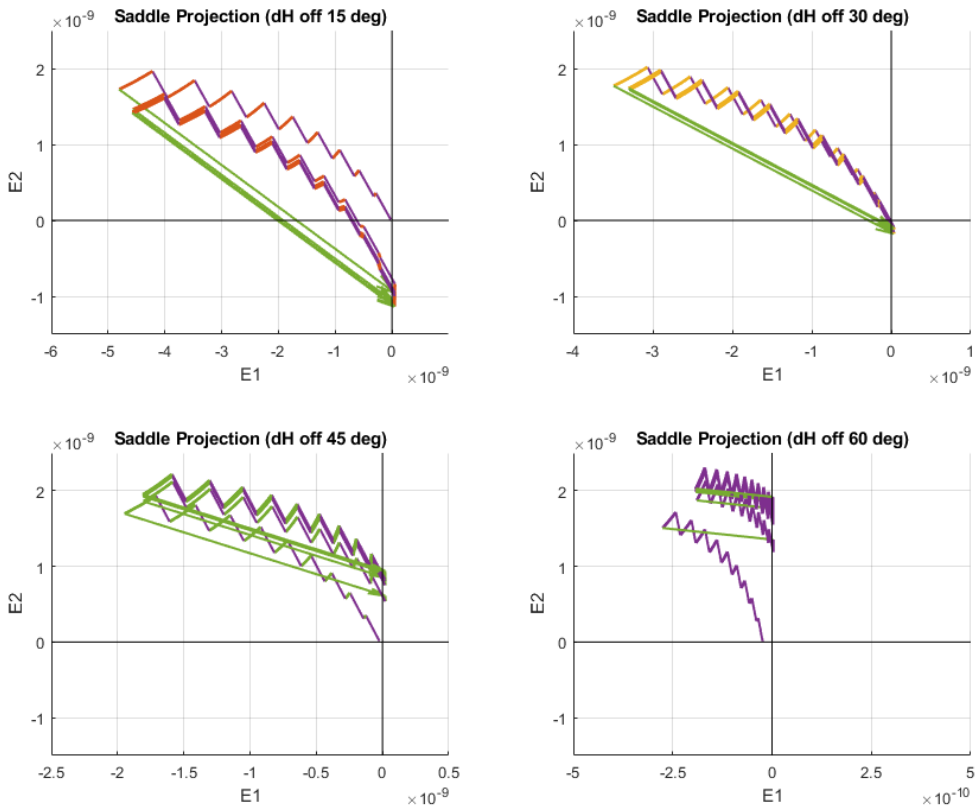

Figure 15. Projection of the trajectory on the saddle plane for different dH/dV strategies, dH 15 deg off RS (top-left) , dH 30 deg off RS (top-right), dH 45 deg off RS (bottom-left) and dH 60 deg off RS (bottom-right). In all plots, the purple lines represent the dH maneuveres and the green lines the dV maneuvers. The spacecraft's trajectory is represented with different colors in every case.

As we have seen, looking at the trajectories in the saddle plane helps understand the impact of changing the direction of maneuvers on the over-all cost of the mission. When the momentum unloads are applied along a fixed direction, this induces a natural drift of the trajectory along that direction. Choosing the direction for the maneuvers to be close to the non-escape direction add small bias along the unstable direction deriving on small station-keeping maneuvers.

CONCLUSION

The size of station-keeping maneuvers depends on many factors like unmodeled perturbation, orbit determination errors, maneuver execution errors, momentum unloads, or the cadence of the maneuvers. In the case of SWFO, the main driver is the frequent momentum unloads, which are all applied along the spacecraft-Sun direction. In this paper we have explored the option of using a different direction for the momentum unloads to minimize their impact on station-keeping.

The CRTBP has been used as a model to describe the motion around a Lissajous orbit, and from the linearized equations of motion around SEL_1 derived what we call the escape and non-escape directions. Maneuvers along the escape directions maximize the variation along the unstable manifold, these are ideal for station-keeping as a small maneuver along the escape direction has a large impact on the instability, and can be used to cancel the natural instability of the orbit at a small

cost. While maneuvers along the non-escape directions should be used for frequent momentum unloads, by definition maneuvers along the non-escape direction do not add to the instability of the orbit.

Monte Carlo simulations have bee performed comparing SWFO's nominal dH/dV strategy (where dH are along the spacecraft-Sun direction) , with a new dH/dV strategy (where dH are along the non-escape direction). In both cases dH are applied every 3 days with the same residual delta-v and station-keeping maneuvers every 30 days. We have seen that this new dH/dV can reduce the delta-v budget for station-keeping up to 90%, being a strategy to be considered for future mission applications.

Finally, a geometric interpretation of the different dH/dV strategies is presented, using the SCC reference frame (similar to the Floquet Modes) to describe the motion close to a Lissajous orbit. Looking at the projection of the different delta-v maneuvers on the saddle plane (defined in the SCC reference) helps understand how different maneuvers affect the escape rate of the trajectories along the unstable manifolds. Using these reference frames to describe the behaviour of the trajectories the delta-v maneuvers can help derive better strategies accounting for the mission constraints.

REFERENCES

[1] C. Simó, G. Gómez, J. Llibre, R. Martínez, and J. Rodríguez, "On the optimal station keeping control of halo orbits," *Acta Astronautica*, Vol. 15, No. 6, 1987, pp. 391–397. Congress of the International Astronautical Federation.

[2] G. G., H. K., M. J., and S. C., "Station-Keeping Strategies for Translunar Libration Point Orbits," *1998 AAS/AIAA Space Flight Mechanics Meeting*, No. Paper AAS 98-168, 1998.

[3] A. Farrés, C. Gao, J. J. Masdemont, G. Gómez, D. C. Folta, and C. Webster, "Geometrical Analysis of Station-Keeping Strategies About Libration Point Orbits," *Journal of Guidance, Control, and Dynamics*, Vol. 45, No. 6, 2022, pp. 1108–1125, 10.2514/1.G006014.

[4] P. J., "L2 Station Keeping Maneuver Strategy for the James Webb Space Telescope," *AAS/AIAA Astrodynamics Specialist Conference*, No. AAS Paper 19-806, 2019.

[5] F. D., P. T., H. K., W. M., and W. W., "Stationkeeping of Lissajous Trajectories in the Earth-Moon System with Applications to ARTEMIS," *AAS/AIAA Spaceflight Mechanics Meeting*, No. AAS Paper 10-113, 2010.

[6] N. Bosanac, C. M. Webster, K. C. Howell, and D. C. Folta, "Trajectory Design for the Wide Field Infrared Survey Telescope Mission," *Journal of Guidance, Control, and Dynamics*, Vol. 42, No. 9, 2019, pp. 1899–1911, 10.2514/1.G004179.

[7] D. Richardson, "A note on a Lagrangian formulation for motion about the collinear points," *Celestial Mechanics*, Vol. 22, 1980, pp. 231—236, 10.1007/BF01229509.

[8] E. Canalias Vila, *Contributions to Libration Orbit Mission Design using Hyperbolic Invariant Manifolds*. PhD thesis, Universitat Politècnica de Catalunya, 2007.